

## **General Disclaimer**

### **One or more of the Following Statements may affect this Document**

- This document has been reproduced from the best copy furnished by the organizational source. It is being released in the interest of making available as much information as possible.
- This document may contain data, which exceeds the sheet parameters. It was furnished in this condition by the organizational source and is the best copy available.
- This document may contain tone-on-tone or color graphs, charts and/or pictures, which have been reproduced in black and white.
- This document is paginated as submitted by the original source.
- Portions of this document are not fully legible due to the historical nature of some of the material. However, it is the best reproduction available from the original submission.

November 1975

Submitted to Phys. Rev. A

(NASA-TM-X-7290C) WIDTHS OF ATOMIC 4s AND  
4p VACANCY STATES, 46 LESS THAN OR EQUAL TO  
Z LESS THAN OR EQUAL TO 50 (NASA) 30 p HC  
\$4.00 CSCL 20

N76-13932

CSCL 20L

Unclassified

~~G3/76 01934~~

## WIDTHS OF ATOMIC 4s and 4p VACANCY STATES, $46 < Z < 50$

Man Hsiung Chen\*† and Bernd Crasemann\*†

NASA Ames Research Center  
Moffett Field, California 94035

Lo I Yin and Tung Tsang\*

## Astrochemistry Branch

Code 691.2, NASA

Goddard Space Flight Center  
Greenbelt, Maryland 20771

Isidore Adler

Department of Chemistry  
University of Maryland  
College Park, Maryland 20742



\* Permanent address: Department of Physics, University of Oregon,  
Eugene, Oregon 97403

<sup>†</sup> Work supported in part by the U.S. Army Research Office - Durham (Grant DAHCO4-75-G-0021) and by the National Aeronautics and Space Administration (Grant NGR 38-003-036).

# National Research Council Senior Research Associate, 1975-76;  
permanent address: Department of Physics, Howard University,  
Washington, D.C. 20059

## Abstract

X-ray photoelectron and Auger spectra involving  $N_1$ ,  $N_2$ , and  $N_3$  vacancy states of Pd, Ag, Cd, In, and Sn were measured and compared with results of free-atom calculations. As previously observed in Cu and Zn Auger spectra that involve 3d-band electrons, we now also find free-atom characteristics, with regard to widths and structure, in the Ag and Cd  $M_4^-N_{4,5}N_{4,5}$  and  $M_5^-N_{4,5}N_{4,5}$  Auger spectra that arise from transitions of 4d-band electrons. Theoretical  $N_1$  widths computed with calculated free-atom Auger energies agree well with measurements. Theory however predicts wider  $N_2$  than  $N_3$  vacancy states (as observed for Xe), while the measured  $N_2$  and  $N_3$  widths are nearly equal to each other and to the average of the calculated  $N_2$  and  $N_3$  widths. The calculations are made difficult by the exceedingly short lifetime of some 4p vacancies and by the extreme sensitivity of super-Coster-Kronig rates, which dominate the deexcitation, to the transition energy and to the fine details of the atomic potential.

## I. INTRODUCTION

The lifetimes of atomic inner-shell vacancies are uniquely related, through the uncertainty principle, to the widths of the corresponding atomic energy levels. In many cases, atomic level widths can be measured quite accurately by x-ray photoelectron spectroscopy,<sup>1,2</sup> providing an important check on calculations of transition probabilities and lending insight into deexcitation processes.<sup>3</sup> In particular, considerable difficulties are still encountered in theoretical estimates of Coster-Kronig rates,<sup>4-6</sup> which often determine the dominant partial widths of states that are characterized by vacancies in the lower L, M, and N subshells<sup>7</sup>; more experimental data are needed as a guide for refined calculations. Available information on atomic level widths is quite incomplete as yet, in spite of its relevance to fundamental theory and applications.<sup>8</sup> In the present paper, we report on measurements of N<sub>1</sub>, N<sub>2</sub>, and N<sub>3</sub> widths in Pd, Ag, Cd, In, and Sn, and compare these with new calculations.

## II. EXPERIMENT

### A. Measurements

The x-ray photoelectron spectrometer used in these experiments has been described previously.<sup>1</sup> Photoelectrons were produced by (nonmonochromatized) Mg K $\alpha_{1,2}$  x rays and retarded to  $\sim$ 100 eV before they entered a 11-cm radius hemispherical electrostatic analyzer. Samples consisted of spectroscopically pure foils. Sample surfaces

were sputter-cleaned with Ar ions until the 1s photoelectron lines of O and C became nondetectable or, at most, barely discernible above background. Spectra were measured at pressures of  $< 5 \times 10^{-8}$  Torr. All measurements were repeated with three different samples of each element.

Lines with favorable signal-to-background ratio were measured at a resolution characterized by 1.1-eV full width at half-maximum (fwhm) of the Au N<sub>7</sub> photoelectron peak. Many N-shell photoelectron lines measured in this work are quite wide (>4 eV), however, and rather weak; in these cases, the spectrometer resolution was reduced to 1.5-eV fwhm for the Au N<sub>7</sub> line, thus enhancing the signal-to-background ratio. Even so, instrumental broadening remained negligible in comparison with the intrinsically large experimental uncertainties associated with such large widths (Sec. IIB).

#### B. Data analysis and results

As in our previous work on M-level widths,<sup>1</sup> the photoelectron spectra were smoothed with a spline-fit computer program. The background on both sides of a peak was fitted with a single fourth-degree polynomial which extends under the peak. Results were drawn with a CalComp-780 plotter. In the 46 < Z < 50 region, the N<sub>2</sub> and N<sub>3</sub> photoelectron lines overlap considerably. Their background-subtracted smooth spectra were deconvoluted with a DuPont 310 curve resolver, subject to the additional criterion that the N<sub>2</sub>/N<sub>3</sub> photoelectron intensity ratio be 1/2. The single-component standard in the curve-resolving process was a Lorentzian shape convoluted with the Gaussian instrumental

contribution, according to the procedure of Wilkinson.<sup>9</sup> The combined width of the vacancy state and the incident x-ray is at least six times the instrumental width in all cases; hence the convoluted shape remains practically Lorentzian.

The application of these procedures to the  $N_{2,3}$  photoelectron spectrum of Ag is illustrated in Fig. 1. The original data, smoothing and computer-fitted background are shown in Fig. 1(a). It is apparent how extensively the wide  $N_2$  and  $N_3$  lines overlap; this makes them difficult to resolve. Moreover, the shape of the spectrum is such that background subtraction involves some degree of subjectivity. The deconvolution of the background-subtracted spectrum, based on Lorentzian line shapes [Fig. 1(b)], is more successful in this case than in some others with poorer signal-to-background ratios and broader peaks. These difficulties, due more to the nature of the photoelectron spectra than to the instrumental resolution, account for the rather large uncertainties attached to some of the measured widths.

Results of the measurements are listed in Table I, with theoretical predictions due to McGuire<sup>10</sup> and from our present calculations. The experimental vacancy-state widths were derived on the assumptions that the width of the Mg  $K\alpha_{1,2}$  x-ray line is 0.8 eV and that the width of the photoelectron line is the Lorentzian sum (simple addition) of the incident x-ray width and the width of the vacancy state. Instrumental broadening is neglected. We believe that it is justifiable to disregard the (Gaussian) instrumental contribution, even at degraded

resolution, because all uncorrected photoelectron lines are at least 3.5 eV wide and allowance for large experimental uncertainties is made in the assigned error limits.

The question remains to what extent non-lifetime broadening<sup>11</sup> contributes to the line widths derived from the x-ray photoelectron spectra. In view of the metallic character of the samples and the large widths (>3.5 eV) under consideration, it is expected that such non-lifetime mechanisms as charging, thermal and phonon broadening, and many-electron (conduction electron) excitations<sup>12-14</sup> do not contribute significantly. Plasma frequencies in the elements studied here correspond to energies<sup>15</sup> of >12 eV and their excitation intensities are generally much lower than those of the main photoelectron peaks, so that broadening due to this cause should be minimal. We have chosen to study only elements with filled d shells, so as to avoid significant broadening due to multiplet splitting and other related final-state effects arising from localized unpaired electrons. Although the precise nature of pronounced shakeup satellites in solids (~5-12 eV) is still somewhat ambiguous, it is an experimental fact that such satellites are observed only in metal compounds and not in the metals themselves.<sup>16-25</sup> Broadening contributions from shakeup or shakeoff satellites should therefore be insignificant in the pure metallic samples used in the present work.

### III. DISCUSSION

#### A. Quasiatomic Auger Spectra

In a previous paper, we have discussed the quasiatomic character of the Auger spectra from solid Cu and Zn.<sup>1</sup> In particular, we showed that the  $L_3$ - $M_{4,5}$  $M_{4,5}$  Auger transition, which involves two electrons from the  $M_{4,5}$  (3d) band of solid Cu and Zn, does not exhibit band structure, but rather, contains fine structure similar to that in spectra of free atoms. In width and shape, these Auger spectra thus differ sharply from the x-ray photoelectron (XPS) spectra of the 3d band itself. The same fine structure has recently been observed in Auger spectra of Zn vapor which contains only free Zn atoms,<sup>26</sup> as well as in solid germanium<sup>27</sup> and in gaseous  $GeH_4$ ,<sup>28</sup> where the 3d electrons are more core-like.

Two reasons exist for this quasiatomic behavior of Auger spectra in contrast to the solid-state character of soft x-ray emission spectra. On the one hand, in the presence of an inner-shell photohole, the more localized valence electrons are likely to be preferentially selected by the Coulomb operator to participate in the Auger process, while the x-ray emission dipole operator has relatively long-range character. On the other hand, the doubly-ionized final state of Auger transitions is more free-atom like than the singly-ionized final state of radiative transitions.<sup>29,30</sup> Our original suggestion<sup>1</sup> concerning a lifetime difference between radiative and radiationless processes is in error, as pointed out by Mehlhorn.<sup>30</sup>

The important physical implications of the quasatomic characteristics of Auger spectra from solids are as follows:

(i) Because Coster-Kronig and Auger transitions are caused by the same Coulomb operator and both lead to doubly-ionized final states, the quasatomic behavior of Auger transitions in solids implies similar behavior of Coster-Kronig transitions.

(ii) In the outer shells, such as the M or N shells of medium-Z elements, the width of a vacancy state is almost entirely governed by Auger and Coster-Kronig transition rates. If these transitions are quasatomic in solids, then the vacancy-state widths as deduced from XPS of solid samples should reflect the quasatomic transition rates, provided that other non-lifetime contributions to the XPS widths are negligible.

(iii) Whereas the fine structure of Auger spectra and the width of photoelectron lines in solids may be quasatomic in character, their kinetic energies, and hence the measured binding energies of electrons in various shells, are definitely not free-atom like, but are influenced by solid-state effects such as extra-atomic relaxation.<sup>31,32</sup>

These points are borne out by the fact that the large discrepancies between theoretically predicted M-vacancy widths<sup>33</sup> and experimentally measured values could be resolved by recalculating the widths using free-atom Auger and Coster-Kronig energies and neutral-atom potentials.<sup>1</sup> We now inquire whether similar free-atom behavior of N Auger spectra exists in metals such as Ag and Cd. Figure 2 shows

the  $M_5-N_{4,5}N_{4,5}$  and  $M_4-N_{4,5}N_{4,5}$  Auger spectra of Ag and Cd and the respective photoelectron spectra of the  $N_{4,5}$  (4d) band. The spectra of In are included for comparison because the In  $N_{4,5}$  level is more core-like. As in the case of Cu and Zn, we note a similarity among the Auger features of Ag and Cd, even though the width and shape of the photoelectron spectra are quite different. The fine structure of these Auger spectra is not well resolved. However, the fine structure is definitely similar to that in the free-atom inner-shell  $M_{4,5}-N_{4,5}N_{4,5}$  Auger spectra of gaseous Xe.<sup>34,35</sup> This similarity was already noted by Aksela<sup>36</sup> under coarse resolution. More recently, Powell conducted a high-resolution study of Ag and specifically emphasized the lack of band structure, and hence, the quasiamionic character of these Auger transitions.<sup>29</sup> Additional evidence for the quasiamionic characteristics is provided by the recently obtained Auger spectrum of Cd vapor,<sup>37</sup> which exhibits similar features as those of Cd metal, although much better resolved. We can thus anticipate that in the  $46 < Z < 50$  range the N-shell widths should be essentially free-atom like. Hence, we compare the measured widths with free-atom calculations.

#### B. Comparison with Theory

##### 1. Calculation of N-subshell widths for quasifree atoms

Free-atom Auger energies, which differ by the extra-atomic relaxation energy from energies measured on solid samples,<sup>32</sup> were calculated from first principles.<sup>1</sup> Rela-

tivistic Hartree-Fock-Slater wave functions were used, with Slater's  $\chi\alpha$  approximation to the exchange correlation term in the expression for the statistical total energy.<sup>38-40</sup> The parameter  $\alpha$  was chosen to be 0.7 throughout. The calculated Coster-Kronig energies are listed in Table II.

Auger and Coster-Kronig transition rates were computed with Herman-Skillman<sup>41</sup> nonrelativistic Hartree-Slater wave functions. The latter tail correction<sup>42</sup> was included, and  $\chi\alpha$  exchange was used. Radiationless transition rates were calculated in  $j-j$  coupling in the standard manner.<sup>5,6</sup> The rates with which we are here concerned are exceedingly sensitive to the atomic potential. This fact is illustrated by the dependence of N-level widths on the choice of exchange potential, as plotted in Fig. 3.

Radiative transitions were disregarded, the radiative partial width of N-shell vacancy states being negligible compared with the radiationless width.<sup>10</sup>

Total widths computed in this manner are included in Table I.

## 2. $N_1$ -level widths

Figure 4 shows that the measured  $N_1$  widths in the  $46 < Z < 50$  region agree exceedingly well with the free-atom calculations. These widths are chiefly determined by the  $N_1-N_{2,3}N_{4,5}$  super-Coster-Kronig rates. Coster-Kronig transition rates are extremely energy-sensitive, particularly near threshold.<sup>1</sup> This fact is well illustrated by the difference between two

sets of results for the  $N_1$  widths obtained by McGuire,<sup>10</sup> who estimated the continuum-electron energy in two different ways; these results differ by a factor of  $\sim 6$  at  $Z=47$  and by  $\sim 25$  at  $Z=50$ . The higher values (not included in Fig. 4), which increase rather than decrease with  $Z$ , were found by estimating the super-Coster-Kronig electron energy  $\epsilon$  through the formula

$$\epsilon = E_{n_1 l_1} (Z) - (1/2) \left[ E_{n_3 l_3} (Z) + E_{n_3 l_3} (Z+1) + E_{n_4 l_4} (Z) + E_{n_4 l_4} (Z+1) \right], \quad (1)$$

where  $E_{n_l} (Z)$ , the binding energy for the  $n_l$  subshell of the neutral atom with nuclear charge  $Ze$ , was taken from the ESCA table of binding energies.<sup>43</sup> The subscript 1 refers to the hole in the initial atom, while 3 and 4 refer to the final holes. The lower set of widths found by McGuire,<sup>10</sup> on the other hand, which agrees well with ours (Fig. 4), was calculated with super-Coster-Kronig energies estimated according to the prescription of Asaad and Burhop<sup>44</sup> with a work-function correction to the ESCA binding energies.<sup>43</sup> Clearly, the latter method of arriving at Coster-Kronig energies is far more realistic.

### 3. $N_{2,3}$ -level widths

Except for  $^{47}\text{Ag}$ , the  $4p_{1/2}-4p_{3/2}$  spin-orbit splitting had not heretofore been resolved in the  $46 < Z < 50$  region. Even though the experimentally resolved  $N_2$  and  $N_3$  peaks are separated by 8 to 15 eV, their widths are comparable with their separation,

causing substantial overlap (Fig. 1). Taking experimental uncertainties into account, however, we find that the measured  $N_2$  and  $N_3$  vacancy-state widths are nearly equal, for each element. Equal  $N_2$  and  $N_3$  widths are also obtained theoretically through McGuire's calculation,<sup>10</sup> in which the  $N_2$  and  $N_3$  levels are assigned the same (average) energy, i.e., spin-orbit energy splitting is neglected. In our own, free-atom calculations, on the other hand, we take account of the difference between  $N_2$  and  $N_3$  binding energies. The widths of the  $N_2$  and  $N_3$  levels in this region are primarily governed by the super-Coster-Kronig transitions  $N_2 - N_4,5$  and  $N_3 - N_4,5$ , which are very energy-sensitive (Fig. 5). Different binding energies for  $N_2$  and  $N_3$  electrons therefore lead to different  $N_2$  and  $N_3$  vacancy-state widths. Somewhat surprisingly, McGuire's calculation<sup>10</sup> which includes a kind of averaging by treating the  $N_2$  and  $N_3$  levels as degenerate, agrees well with our measurements (Figs. 6 and 7; Table I). Our calculation, on the other hand, leads to  $N_2$  widths that are too large and to  $N_3$  widths that are too small, in general, compared with experiment. The average of our theoretical  $N_2$  and  $N_3$  widths does, however, agree with the (nearly equal) measured  $N_2$  and  $N_3$  widths. In view of the good agreement of our calculated  $N_1$  widths with measurement, the discrepancy in the  $N_2$  and  $N_3$  widths is puzzling. We note that the large (59.5-eV)  $N_2$  width that we calculate for Xe (Table I) is not contrary to observation: in ESCA measurements, it was

found that the  $N_2$  level of Xe is far too broad for positive identification.<sup>34</sup>

#### 4. $N_{4,5}$ -level widths

The  $N_{4,5}$  levels form the 4d band of Ag and Cd and are not split in In or Sn (Fig. 2). No effort was therefore made to measure the individual widths of these levels for comparison with atomic calculations.

#### 5. Concluding Remarks

The following difficulties are encountered in the calculation of theoretical N-level widths:

1. The super-Coster-Kronig transition rates which largely govern the widths are exceedingly energy-sensitive.
2. These radiationless transition rates are extraordinarily sensitive to the fine details of the atomic potential.
3. The very short lifetime of the  $N_{2,3}$  hole states casts some doubt upon the basic validity of perturbation theory to calculate the decay of these states.

#### ACKNOWLEDGMENTS

Two of us (M.H.C. and B.C.) wish to thank Hans Mark, Director of the NASA Ames REsearch Center, and his colleagues for their hospitality at the Center. We take pleasure in acknowledging the able assistance of W. Lew in performing the experiments. At Howard University this research was supported by NASA Grant NGR 09-011-057. At the University of Maryland this research was supported by the Center of Materials Research.

<sup>1</sup>L. I Yin, I. Adler, T. Tsang, M. H. Chen, D. A. Ringers, and B. Crasemann, Phys. Rev. A 9, 1070 (1974).

<sup>2</sup>M. O. Krause, in Atomic Inner-Shell Processes, edited by B. Crasemann (Academic, New York, 1975), Vol. 2, p. 33.

<sup>3</sup>L. I Yin, T. Tsang, and I. Adler, Physica Fennica 9, S1, 256 (1974).

<sup>4</sup>L. I Yin, I. Adler, M. H. Chen, and B. Crasemann, Phys. Rev. A 7, 897 (1973).

<sup>5</sup>M. H. Chen, B. Crasemann, and V. O. Kostroun, Phys. Rev. A 4, 1 (1971).

<sup>6</sup>B. Crasemann, M. H. Chen, and V. O. Kostroun, Phys. Rev. A 4, 2161 (1971).

<sup>7</sup>E. J. McGuire, in Atomic Inner-Shell Processes, edited by B. Crasemann (Academic, New York, 1975), Vol. 1, p. 293.

<sup>8</sup>O. Keski-Rahkonen and M. O. Krause, At. Data Nucl. Data Tables 14, 139 (1974).

<sup>9</sup>D. H. Wilkinson, Nucl. Instrum. Methods 95, 259 (1971).

<sup>10</sup>E. J. McGuire, Phys. Rev. A 9, 1840 (1974) and Sandia Laboratories Report No. SAND-75-0443 (1975), unpublished.

<sup>11</sup>P. H. Citrin, P. M. Eisenberger, W. C. Marra, T. Åberg, J. Utriainen, and E. Källne, Phys. Rev. B 10, 1762 (1974).

<sup>12</sup>S. Doniach and M. Sunjic, J. Phys. C 3, 285 (1970).

<sup>13</sup>P. H. Citrin, Phys. Rev. B 8, 5545 (1973).

<sup>14</sup>S. Hüfner and G. K. Wertheim, Phys. Rev. B 10, 3197 (1974).

<sup>15</sup>D. Pines, Rev. Mod. Phys. 28, 184 (1956).

<sup>16</sup>T. Novakov, Phys. Rev. B 3, 2693 (1971); T. Novakov and R. Prins, Solid State Commun. 9, 1975 (1972).

<sup>17</sup>A. Rosencwaig, G. K. Wertheim, and H. J. Guggenheim, Phys. Rev. Lett. 27, 479 (1971).

<sup>18</sup>D. C. Frost, A. Ishitani, and C. A. McDowell, Mol. Phys. 24, 861 (1972).

<sup>19</sup>L. J. Matienzo, W. E. Swartz, Jr., and S. O. Grim, Inorg. Nucl. Chem. Lett. 8, 1085 (1972).

<sup>20</sup>L. J. Matienzo, L. I. Yin, S. O. Grim, and W. E. Swartz, Jr., Inorg. Chem. 12, 2762 (1973).

<sup>21</sup>C. A. Tolman, W. M. Riggs, W. J. Linn, C. M. King, and R. C. Wendt, Inorg. Chem. 12, 2770 (1973).

<sup>22</sup>K. S. Kim. J. Electron Spectroscopy 3, 217 (1974).

<sup>23</sup>G. K. Wertheim, R. L. Cohen, A. Rosencwaig, and H. J. Guggenheim, in Electron Spectroscopy, edited by D. A. Shirley (North-Holland, Amsterdam, 1972), p. 813.

<sup>24</sup>A. J. Signorelli and R. G. Hayes, Phys. Rev. B 8, 81 (1973).

<sup>25</sup>T. Robert and G. Offergeld, Chem. Phys. Lett. 29, 606 (1974).

<sup>26</sup>S. Aksela and H. Aksela, Phys. Lett. 48A, 19 (1974); S. Aksela, J. Väyrynen, and H. Aksela, Phys. Rev. Lett. 33, 999 (1974).

<sup>27</sup>I. Lindau and C. C. Ribbing, *Phys. Stat. Sol.* 59, 259 (1973); *Phys. Lett.* 44A, 509 (1973).

<sup>28</sup>W. B. Perry and W. L. Jolly, *Chem. Phys. Lett.* 23, 529 (1973).

<sup>29</sup>C. J. Powell, *Phys. Rev. Lett.* 30, 1179 (1973).

<sup>30</sup>W. Mehlhorn, *Physica Fennica* 9, S1, 223 (1974).

<sup>31</sup>D. A. Shirley, *Chem. Phys. Lett.* 17, 512 (1972); *Chem. Phys. Lett.* 15, 185 (1972).

<sup>32</sup>S. P. Kowalczyk, R. A. Pollak, F. R. McFeely, L. Ley, and D. A. Shirley, *Phys. Rev. B* 8, 2387 (1973).

<sup>33</sup>E. J. McGuire, *Phys. Rev. A* 5, 1043 (1972); *Phys. Rev. A* 5, 1052 (1972).

<sup>34</sup>K. Siegbahn, C. Nordling, G. Johansson, J. Hedman, P. F. Hedén, K. Hamrin, U. Gelius, T. Bergmark, L. O. Werme, R. Manne, and Y. Baer, ESCA Applied to Free Molecules (North-Holland, Amsterdam, 1969), p. 49.

<sup>35</sup>S. Hagmann, G. Hermann, and W. Mehlhorn, *Z. Phys.* 266, 189 (1974).

<sup>36</sup>S. Aksela, *Z. Phys.* 244, 268 (1971).

<sup>37</sup>H. Aksela and S. Aksela, *J. Phys. B* 7, 1262 (1974).

<sup>38</sup>J. C. Slater, in Advances in Quantum Chemistry, edited by P. O. Löwdin (Academic, New York, 1972), Vol. 6.

<sup>39</sup>J. C. Slater, Quantum Theory of Molecules and Solids, Vol. 4: The Self-Consistent Field for Molecules and Solids (McGraw-Hill, New York, to be published).

<sup>40</sup> J. C. Slater, J. Phys. Paris 33, C3-1 (1972).

<sup>41</sup> F. Herman and S. Skillman, Atomic Structure Calculations  
(Prentice-Hall, Englewood Cliffs, N. J., 1963).

<sup>42</sup> R. Latter, Phys. Rev. 99, 510 (1955).

<sup>43</sup> K. Siegbahn, C. Nordling, A. Fahlman, R. Nordberg, K. Hamrin,  
J. Hedman, G. Johannson, T. Bergmark, S. Karlsson, I.  
Lindgren, and B. Lindberg, ESCA, Atomic, Molecular, and  
Solid State Structure Studied by Means of Electron  
Spectroscopy (Almqvist and Wiksells, Uppsala, 1967),  
Appendix 1.

<sup>44</sup> W. N. Asaad and E. H. S. Burhop, Proc. Phys. Soc. (London)  
71, 369 (1958).

Table 1. Theoretical and experimental widths  $\Gamma(N_i)$  of  $N_i$ -subshell vacancy states (in ev).

| Element | $\Gamma(N_1)$ |               | $\Gamma(N_2)$ |              | $\Gamma(N_3)$ |              |
|---------|---------------|---------------|---------------|--------------|---------------|--------------|
|         | Theory        |               | Theory        |              | Theory        |              |
|         | a             | b             | a             | b            | a             | b            |
| 46 Pd   | 5.25          | $5.0 \pm 0.5$ | 7.79          | $6.5 \pm 1$  | 6.32          | $6.5 \pm 1$  |
| 47 Ag   | 41.9 (7.0)    | 4.13          | 4.2 $\pm$ 0.5 | 9.69         | 10.55         | $8.5 \pm 1$  |
| 48 Cd   | 4.07          | $4.0 \pm 0.5$ | 13.38         | $12 \pm 1.5$ | 8.65          | $10 \pm 1.5$ |
| 49 In   | 3.03          | $3.5 \pm 0.5$ | 17.59         | $15 \pm 2$   | 10.55         | $14 \pm 2$   |
| 50 Sn   | 78.2 (3.1)    | 2.89          | $2.8 \pm 0.5$ | 16.2         | 20.81         | $17 \pm 2$   |
| 54 Xe   |               | 5.87          |               | 59.48        |               | 2.38         |

a McGuire (Reference 10). Values in brackets are based on an alternative energy estimate for the  $N_1-N_2,3N_4,5$  super-Coster-Kronig transitions. See text, Sec. III B2.

b Present free-atom calculations.

Table II. Theoretical N Coster-Kronig and super-Coster-Kronig transition energies from free-atom calculations (in eV).

| Element | $N_2 N_{45}$ | $N_3 N_{45}$ | $N_2 O_1$ | $N_2 O_{23}$ | $N_3 O_1$ | $N_3 O_{23}$ | $N_{45} N_{45}$ | $N_{45} N_{45}$ | $N_{45} N_{45}$ |
|---------|--------------|--------------|-----------|--------------|-----------|--------------|-----------------|-----------------|-----------------|
| 46 Pd   | 11.45        | 15.74        |           |              |           |              | 63.17.          | 30.53           | 26.24           |
| 47 Ag   | 7.82         | 11.57        | 18.20     |              | 21.95     |              | 64.27           | 29.74           | 25.99           |
| 48 Cd   | 4.60         | 10.60        | 18.21     |              | 24.21     |              | 66.16           | 29.38           | 23.38           |
| 49 In   | 5.02         | 16.77        | 24.48     | 23.70        | 31.41     | 65.91        | 27.64           | 20.71           |                 |
| 50 Sn   |              | 15.01        | 23.48     | 22.84        | 31.31     | 63.10        | 24.27           | 16.47           |                 |
| 54 Xe   | 21.10        | 32.52        | 34.66     | 46.08        | 61.23     |              | 6.23            |                 |                 |

## Figure Captions

Fig. 1.  $Mg\ K\alpha_{1,2}$  x-ray excited photoelectron spectrum of Ag. (a) Original spectrum with smoothing and computer-fitted background. (b) Deconvolution of the background-subtracted spectrum into Lorentzian shapes produced with a DuPont 310 curve resolver, subject to the criterion that the  $N_2/N_3$  intensity ratio be 1/2. Units on the abscissa are 0.4 eV/channel.

Fig. 2.  $M_4-N_4,5$  and  $M_5-N_4,5$  Auger spectra (left) and  $Mg\ K\alpha$  x-ray excited  $N_{4,5}$  photoelectron spectra (right) of Ag, Cd, and In. The small peak in the  $N_{4,5}$  photoelectron spectra is caused by the  $Mg\ K\alpha_{3,4}$  satellite radiation from the x-ray source.

Fig. 3. Dependence of the  $N_1$ - and  $N_3$ -level widths on the choice of exchange used in the calculation, illustrating extreme sensitivity of the dominant radiationless transition rates to the atomic potential.

Fig. 4. Comparison of theoretical and experimental widths of  $N_1$  vacancy states. Experimental data and free-atom calculations are from the present work; triangles represent the lower of two sets of results obtained by McGuire (Reference 10) under different energy assumptions (see text, Sec. III B 2).

Fig. 5  $N_2-N_4N_5$  and  $N_3-N_4N_5$  partial widths of Sn as functions of Auger electron energy, illustrating steep energy dependence of these super-Coster-Kronig transition rates.

Fig. 6. Comparison of measured  $N_2$ -level widths with theoretical results from the present work and of McGuire (Reference 10).

Fig. 7. Comparison of measured  $N_3$ -level widths with theoretical results from this work and of McGuire (Reference 10)

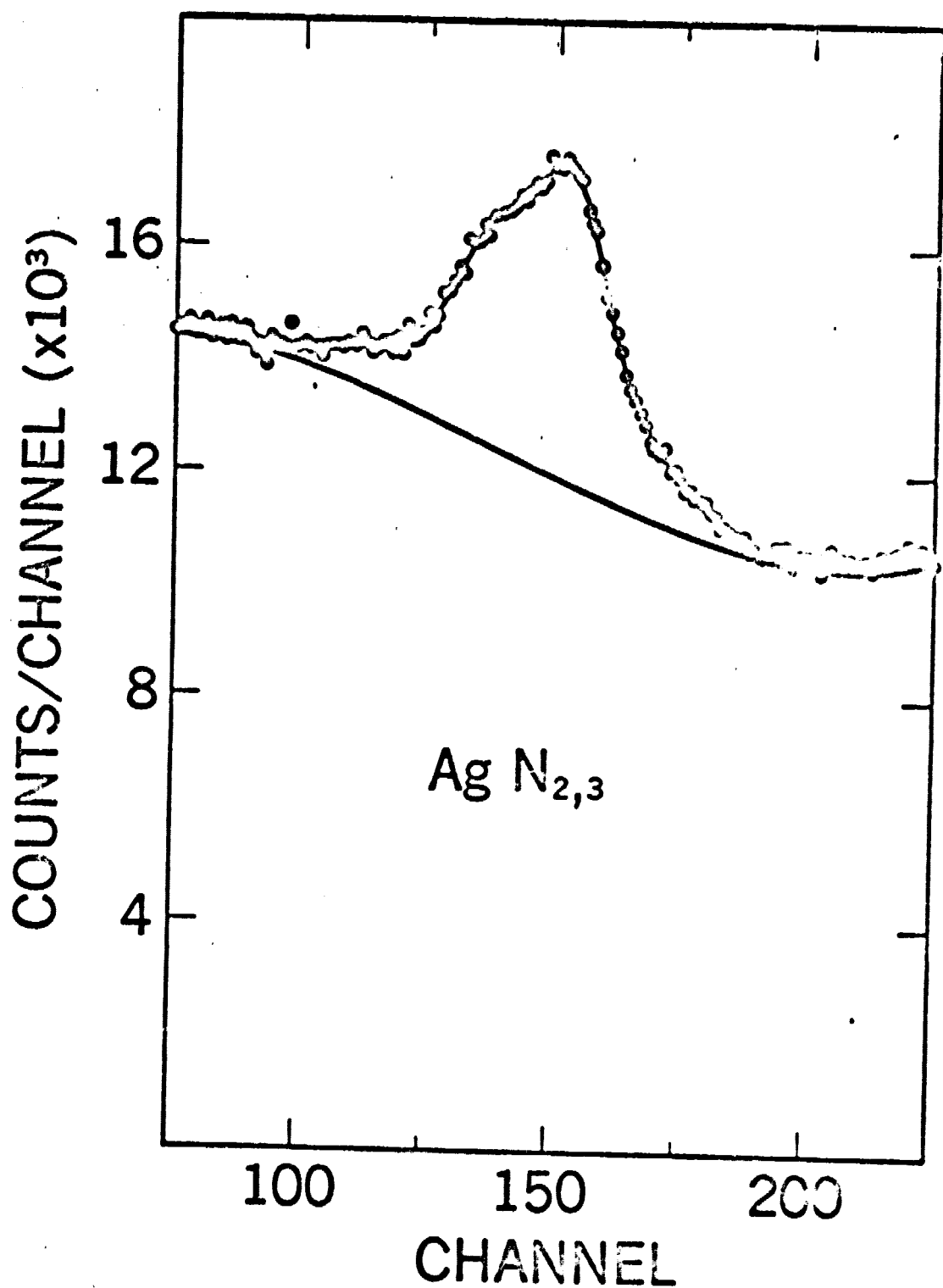


Fig. 1A

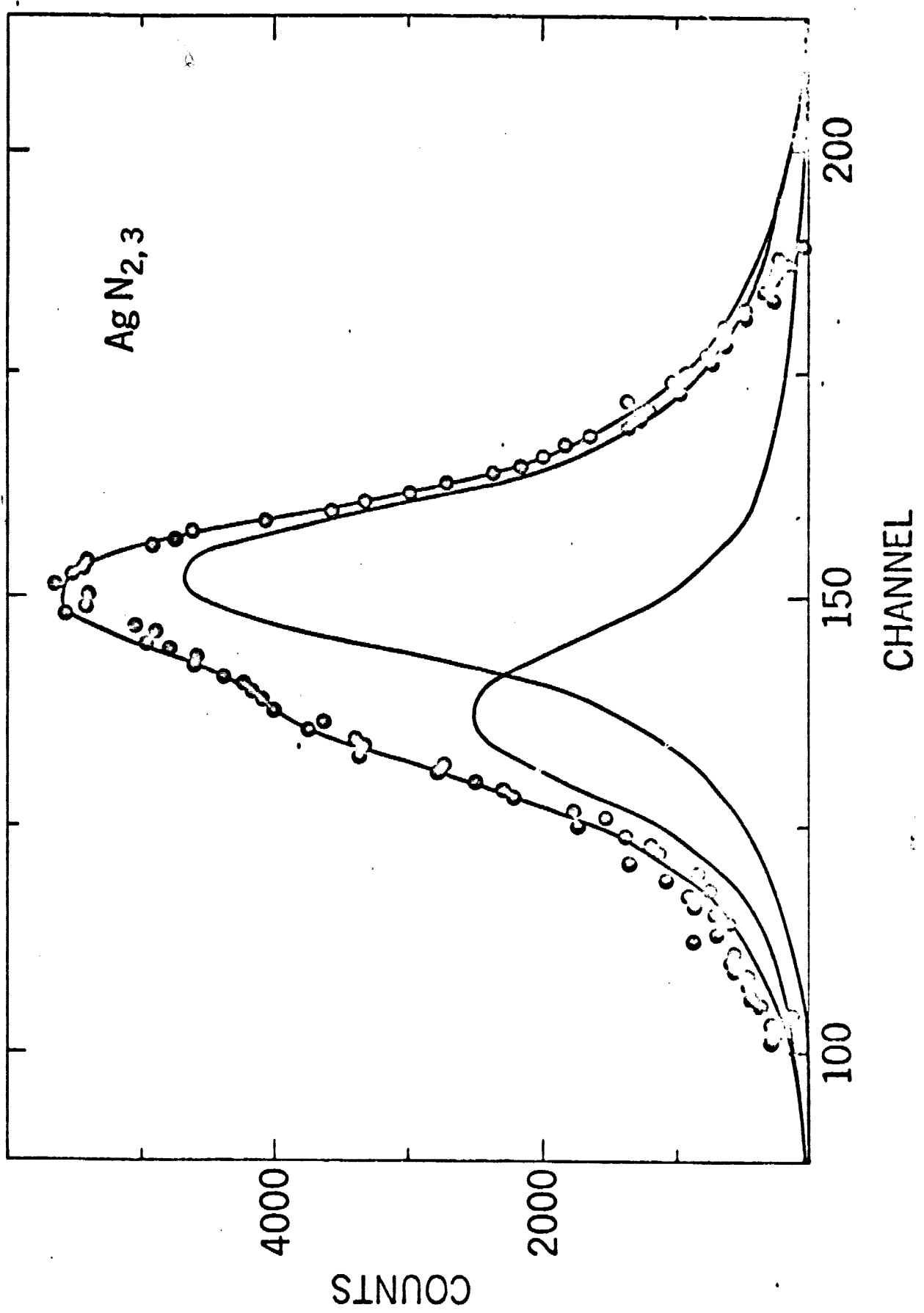
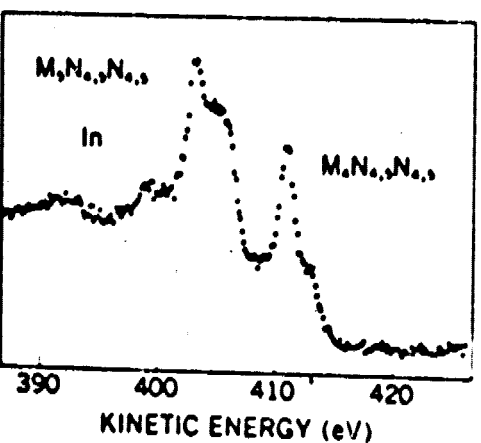
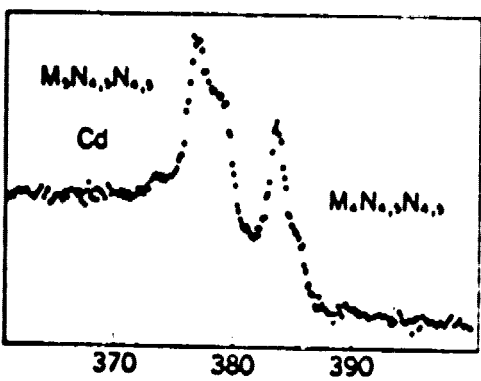
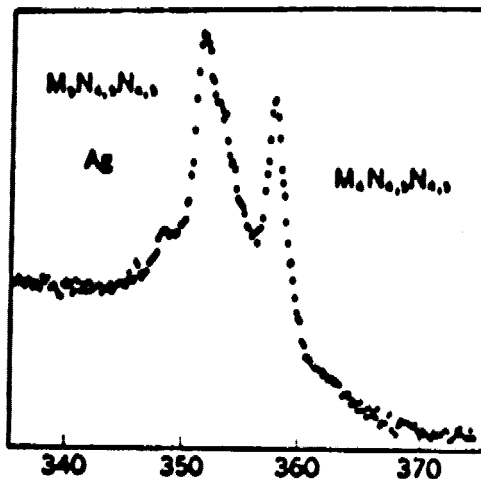


Fig. 1 (b)

COUNTS/CHANNEL (ARBITRARY)



PAGE 10  
OF 10  
QUALITY

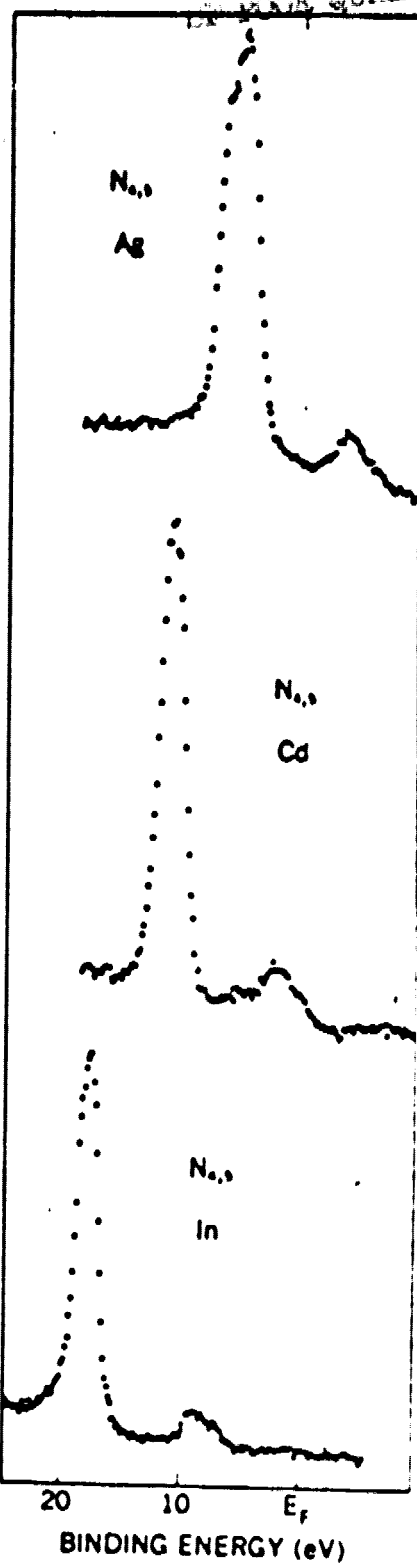


Fig. 2

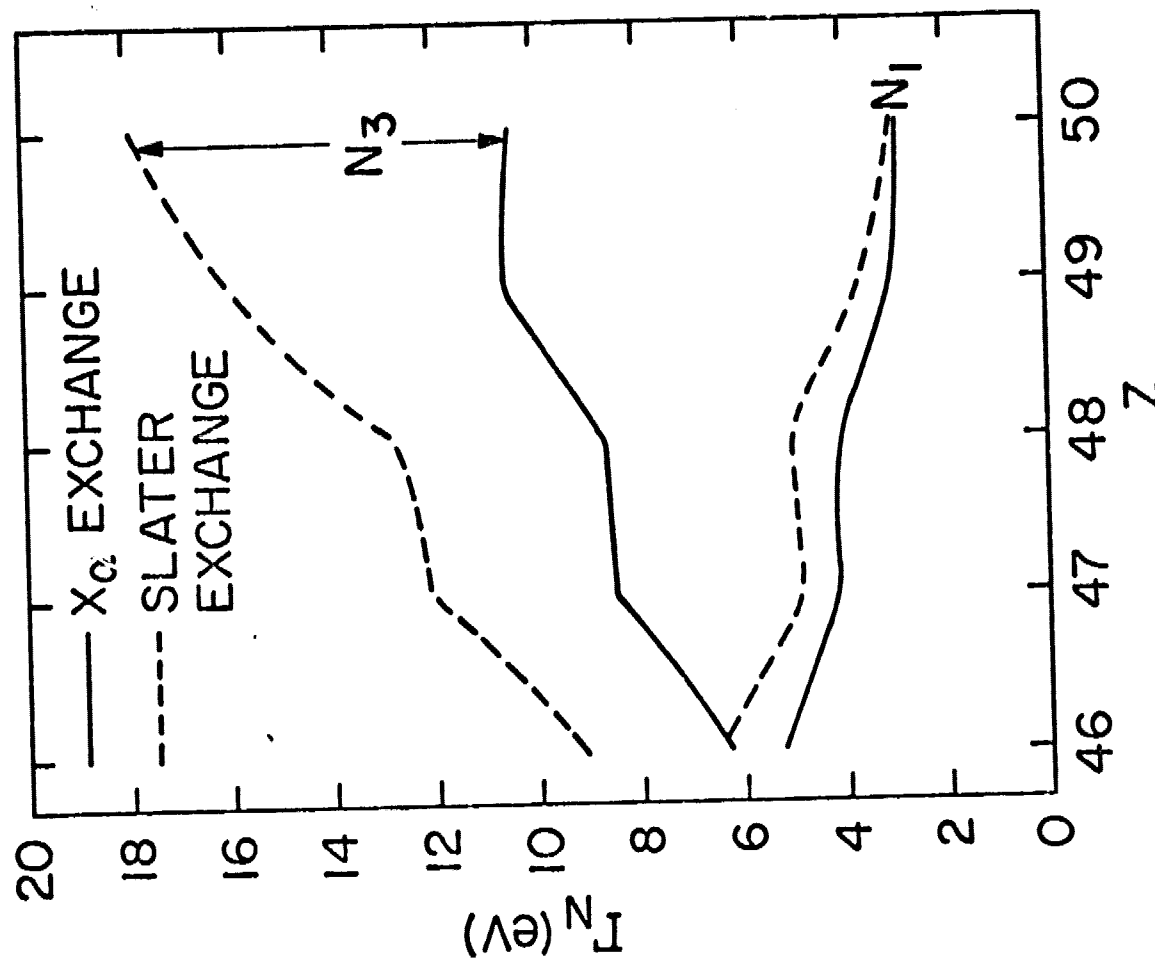


FIG. 3

ORIGINAL  
OF POOR QUALITY

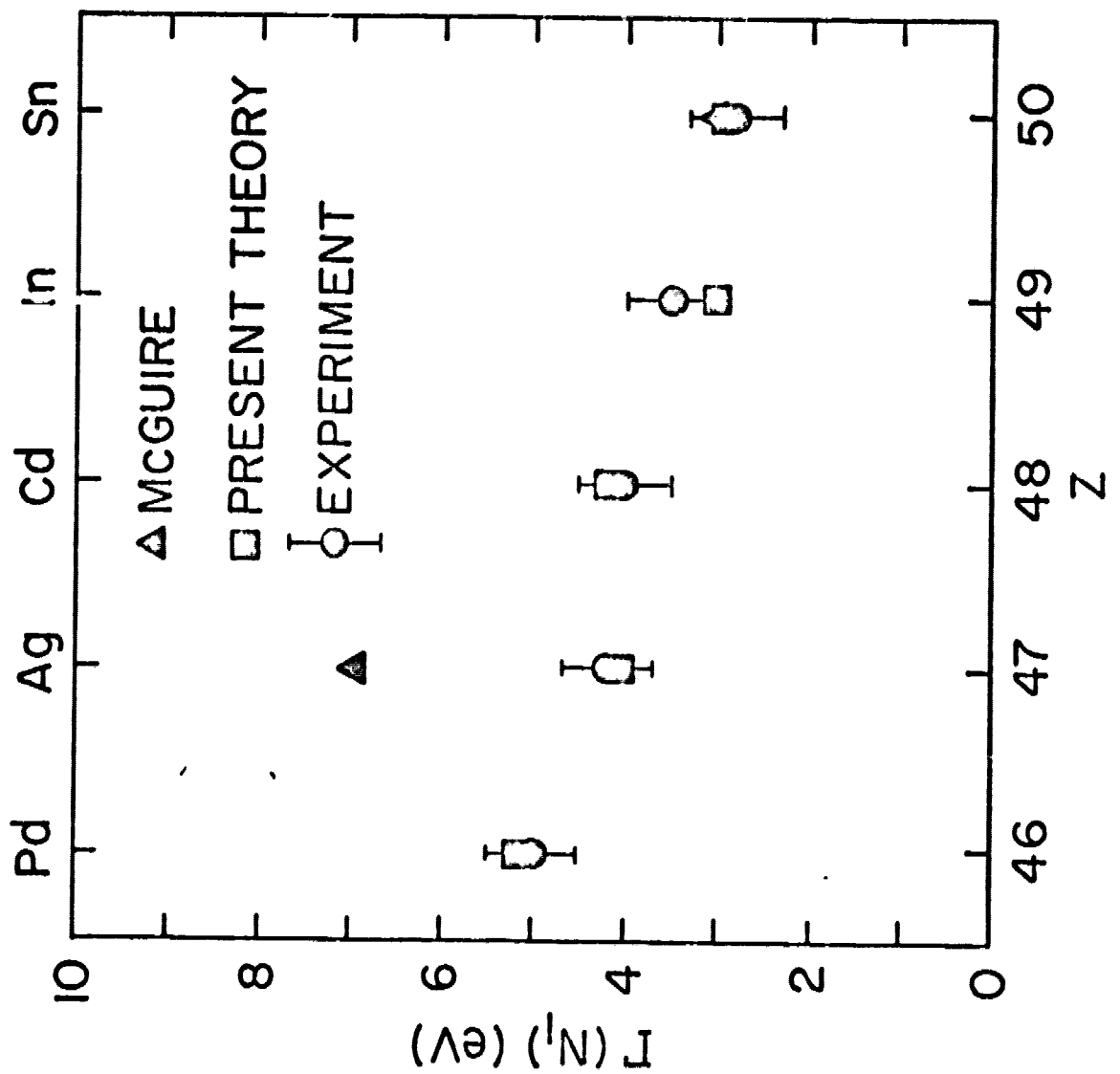
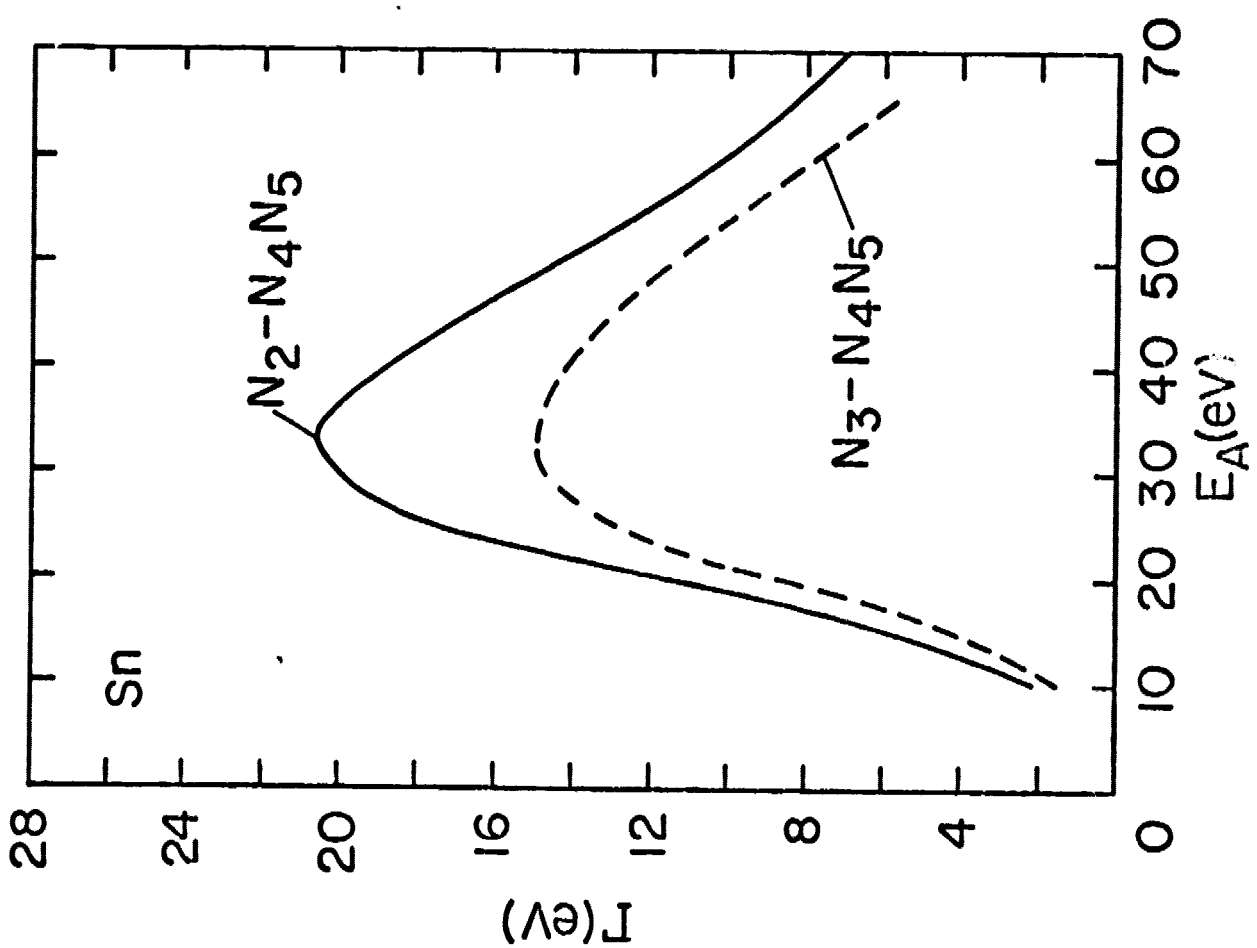


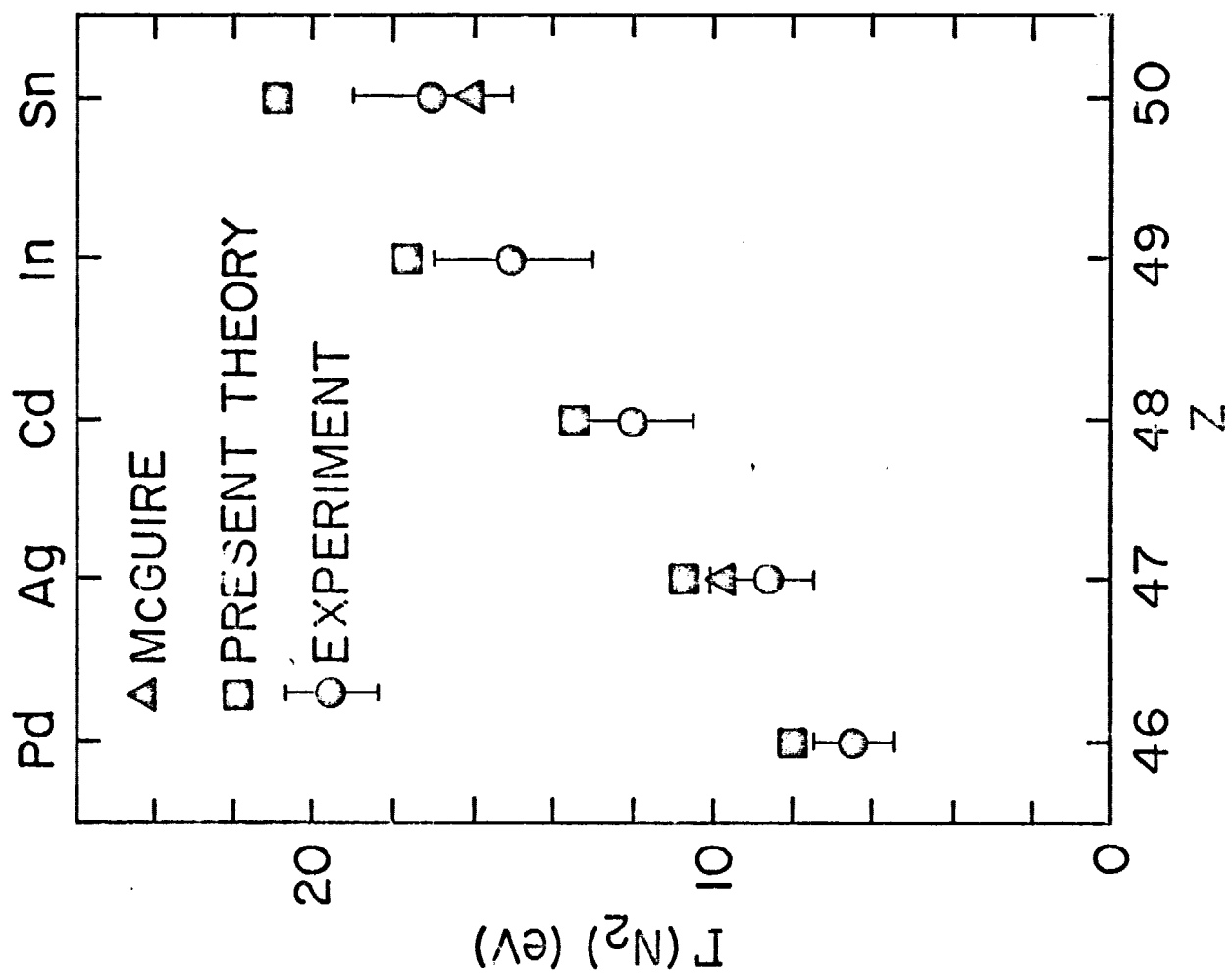
Fig. 4

Fig. 5



ORIGINAL PAGE IS  
OF POOR QUALITY

Fig. 6



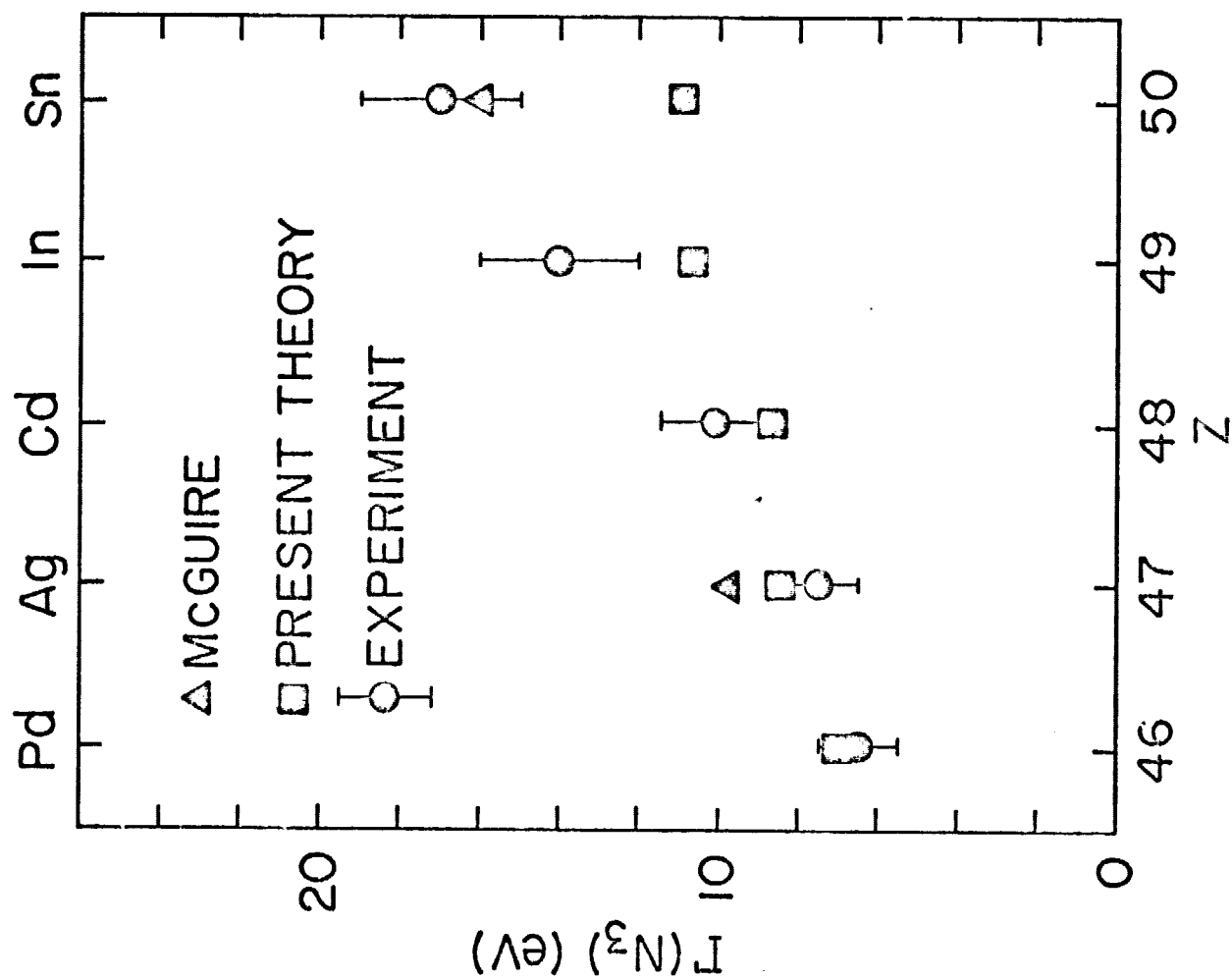


FIG. 7